Polymer Chemistry

Cite this: *Polym. Chem.*, 2012, **3**, 2852

www.rsc.org/polymers

PAPER

Preparation of monolithic superparamagnetic nanoparticle–polymer composites using a polymerizable acetylacetonate and magnetite nanoparticles†

David A. Marsh,‡ Megan W. Szyndler,‡ Robert M. Corn* and A. S. Borovik*

Received 5th May 2012, Accepted 18th July 2012
DOI: 10.1039/c2py20304a

The formation of nanoparticle-polymer composites that can be processed by injection molding from superparamagnetic magnetite (Fe_3O_4) nanoparticles (MNPs) and the polymerizable molecule styryl acetylacetonate (stacac) is described. The best composites were created by first synthesizing MNPs in the presence of a surfactant followed by replacement with an excess of stacac monomer in a surfactant exchange reaction. Polymerization of the stacac–MNP mixture produced a dense packing of nanoparticles within a polymer matrix, resulting in a magnetic, monolithic material that was characterized with a combination of transmission electron microscopy (TEM), Fourier transform infrared absorption spectroscopy (FTIR), powder X-ray diffraction (XRD) and vibrating sample magnetometry (VSM). The material exhibited superparamagnetic properties similar to pure MNP samples, albeit with a lower total magnetic saturation. An advantage of this polymer-based composite material is its ability to be processed with methods such as mold-casting or microfluidics into a variety of 3-dimensional structures (*e.g.*, toroids) for different electronics applications.

Introduction

Metal (Fe, Co, Ni) and metal oxide nanoparticles often exhibit magnetic properties that are potentially useful in a variety of applications including the fabrication of high frequency electronic and magnetic devices.[1–3] A common challenge in the preparation of functional magnetic materials from these nanoparticles is how to control the assembly of the nanoparticles into three-dimensional structures: specific nanoparticle spacing and density are often needed to achieve an optimally functional device. One approach towards the development of more functional systems is to prepare composite materials composed of nanoparticles encapsulated within a polymeric matrix. These types of polymer–nanoparticle composites are advantageous because conventional processing methods for polymers can be utilized that are not compatible with nanoparticles.[4,5] For example, with polymeric materials, the possible approaches for device fabrication can be extended to injection molding[6] and microfluidic techniques,[7] which allow for specific control over the size and shape of the resulting device.

Ideally these types of composite materials would retain the desirable physical properties of the nanoparticles upon inclusion within a polymer matrix. However, this is often difficult to achieve because the matrix usually does not contribute to the physical properties associated with the nanoparticles. For example, composite materials containing an organic polymer and magnetic nanoparticles exhibit lower saturation magnetization than that of the pure nanoparticles.[5,8] Therefore, synthetic methods are still needed that produce composite materials having properties approaching those found in nanoparticles.

In this report we demonstrate a polymeric composite that can be molded homogeneously with only a moderate loss of magnetic properties. Two methods are described for the synthesis of materials composed of magnetite (Fe_3O_4) nanoparticles (MNPs) embedded within a polystryene matrix. A surfactant exchange method involved the treatment of MNPs with a monomer composed of both a polymerizable styrene moiety and a bidentate metal binding site, 3-((4-vinylphenyl)methyl)pentane-2,4-dione (stacac). A different method utilized a new monomeric iron(III) complex, $Fe(stacac)_3$, that was designed as a synthon to prepare MNPs. We characterized the MNPs and their corresponding MNP-composite material with a combination of transmission electron microscopy (TEM), Fourier transform infrared absorption spectroscopy (FTIR), powder X-ray diffraction (XRD) and vibrating sample magnetometry (VSM) measurements. The MNP-composite material exhibited superparamagnetic properties similar to pure MNP samples, albeit with a lower total magnetic saturation. We were able to fabricate the MNP-composite material within a Teflon mold to generate a reproducible shape, demonstrating one possible method of processing this material.

Department of Chemistry, University of California-Irvine, Irvine, CA 92697, USA. E-mail: rcorn@uci.edu; aborovik@uci.edu

† Electronic supplementary information (ESI) available. See DOI: 10.1039/c2py20304a

‡ These authors contributed equally to this work.

Experimental

Materials

All reagents and solvents were purchased from commercial sources and were used as received unless otherwise noted. Sodium acetylacetonate was prepared according to literature procedures.[9]

Physical methods

Transmission electron microscopy images were taken on a FEI/Philips CM-20 conventional TEM at a voltage of 200 kV. X-ray powder diffraction patterns were obtained on a Rigaku Ultima III powder diffractometer with graphite monochromatized Cu Kα radiation (λ = 1.54178 Å). Infrared spectra were recorded with a Varian 800 FT-IR Scimitar series spectrophotometer. The syntheses of all metal complexes were conducted in a Vacuum Atmosphere dry box under an argon atmosphere. ^{1}H NMR spectra were recorded on a Bruker GN500 spectrometer. Absorbance spectra were recorded with a Cary 50 spectrophotometer using a 0.01 cm quartz cuvette. X-band electron paramagnetic resonance (EPR) spectra were recorded at 77 K with a Bruker EMX spectrometer.

Magnetic measurements

Magnetic properties were measured with a Quantum Design MPMS SQUID-VSM. Vibrating sample magnetometry data were taken in the range of −10 000 Oe (−1 Tesla) to +10 000 Oe (+1 Tesla). The magnetization saturation value (M_{sat}) was the maximum magnetization observed, and was taken at 10 000 Oe. The analysis of the volume magnetic susceptibility (χ), the response of the material to the applied magnetic field, used SI units for volume magnetization (M) and applied magnetic field ($\boldsymbol{H}$), which resulted in a linear relationship between M and $\boldsymbol{H}$. Note that the conversion of M from mass to volume magnetization used a density value for Fe_3O_4 of 5.2 g cm^{-3}. After unit conversion, the susceptibility was found by taking the slope about zero. The coercivity values (H_c), the amount of applied magnetic field required to return the material to zero magnetization, were calculated as the average of the two values for $\boldsymbol{H}$ when $M = 0$ in the hysteresis curve. Note: The reported numbers for the control experiment are an average of 4 unique samples.

Synthesis of 3-((4-vinylphenyl)methyl)pentane-2,4-dione (stacac)[10]

Modified from literature procedures, sodium acetylacetonate (3.33 g, 23.8 mmol) and 1,4-pentanedione (2.38 g, 23.8 mmol) were dissolved in a mixture of dimethylformamide (10 mL) and acetonitrile (20 mL). Under N_2 atmosphere, 4-vinylbenzylchloride (3.35 mL, 23.8 mmol) was added *via* syringe, after which the mixture was treated with NaI (0.120 g, 0.795 mmol) and heated to 80 °C. After 2 h of stirring, the mixture was allowed to cool to room temperature, H_2O (75 mL) was added, the product was extracted with toluene (3 × 50 mL), washed once each with H_2O (50 mL) and brine (50 mL), dried over Na_2SO_4, and filtered. The filtrate was concentrated under reduced pressure to afford an orange oil. The crude product was further purified by column chromatography (SiO_2, 3 : 1 hexanes : ethyl acetate) yielding a pale orange oil. Yield: 94%. ^{1}H NMR (500 MHz, $CDCl_3$, δ, ppm): 7.28–7.36 (m, 2H, Ar*H*), 7.10–7.12 (m, 2H, Ar*H*), 6.68 (dd, 1H, ArC*H*=CH$_2$), 5.71 (d, 1H, CH=C*H*), 5.22 (d, 1H, CH=C*H*), 4.00 (t, 0.34H, (CO)$_2$C*H*CH$_2$ keto-form), 3.65 (s, 0.92H, ArCH_2C enol-form), 3.13 (d, 0.70H, ArCH_2CH keto-form), 2.07 (s, 6H, COCH$_3$). ^{13}C NMR ($CDCl_3$, δ, ppm): 23.30, 29.73, 32.70, 33.98, 69.95, 108.19, 113.51, 113.80, 126.54, 126.57, 128.81, 136.33, 136.39, 139.32, 191.93, 203.49. FTIR (salt plates, cm^{-1}): 1700 (CO).

Synthesis of Fe(stacac)$_3$

Stacac (409 mg, 1.89 mmol) was dissolved in diethyl ether (5 mL), KH (74 mg, 1.9 mmol) was added in one portion, and the reaction was allowed to stir for 2 h. Solid K(stacac) was formed and isolated by filtration: the solid was further washed with diethyl ether and dried under vacuum. In a separate container, $FeCl_3$ (70. mg, 0.43 mmol) was dissolved in diethyl ether (5 mL) and the mixture was treated with K(stacac) (329 mg, 1.23 mmol), causing a color change from green to red. The reaction was allowed to stir at room temperature for 2 h, the solution was then filtered to remove KCl, and the solid was washed with diethyl ether. The filtrate was concentrated under reduced pressure and the residue was washed with cold pentane to yield 140 mg of Fe(stacac)$_3$ as a shiny dark red solid. Yield: 46%. Anal. calcd for Fe(stacac)$_3$·H_2O, $C_{42}H_{47}FeO_7$: C, 70.10; H, 6.58%. Found: C, 70.54; H, 6.33%. FTIR (KBr pellet, cm^{-1}): 1569 (CO). EPR (X-band, DCM/toluene, 77 K): g = 4.3. UV-Vis (THF) λ_{max}, nm (ε, cm^{-1} M^{-1}): 462 (4204), 368 (sh).

Synthesis of Fe_3O_4 nanoparticles (MNPs)[11]

Fe(acac)$_3$ (1.06 g, 3.00 mmol) or Fe(stacac)$_3$ (2.10 g, 3.00 mmol) was dissolved in 30 mL absolute ethanol. A mixture of methyl hydrazine (0.655 mL, 12.0 mmol) and deionized water (4.32 mL, 80.0 mmol) dissolved in 10 mL ethanol was added dropwise to the solution at room temperature. The mixture was brought to reflux, at which point a black precipitate forms, and refluxing continued for 24 h. The solid was washed with absolute ethanol (×3) and collected by centrifugation (12 000 rpm, 5 min).

Synthesis of MNP-composite material

Fe_3O_4 nanoparticles (50 mg), a 1 M solution of monomer (either stacac, styrene, or EGDMA) in absolute ethanol (300 μL) and AIBN (5 mg, 0.03 mmol) were dissolved in absolute ethanol (2 mL) within a 20 mL scintillation vial, and sonicated for 15 min. Volatiles were removed under reduced pressure, and then 400 μL absolute ethanol was added and the mixture was sonicated for another 15 min to yield a viscous liquid. The solution was transferred to a Teflon mold open to air and heated at 80 °C for 30 min, at which point a solid monolithic material was formed.

Results and discussion

Surfactant design

The preparation of nanoparticle-composite materials employed the multifunctional compound stacac (Scheme 1),[10] which is a

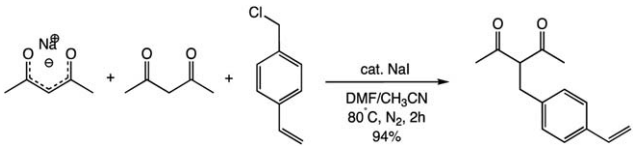

Scheme 1 Synthesis of stacac.

bidentate ligand that binds metals through the acetylacetonate unit.

Unlike the more common acetylacetone (acac) ligand, stacac also contains a polymerizable styrene group that potentially can be used to form cross-linked materials. We investigated exchanging surfactant molecules on MNPs: replacement of the surface bound ligands with stacac would afford MNPs that could be polymerized into the desired composite materials. In addition, we studied formation of MNPs with $Fe(stacac)_3$ and examined their physical and chemical properties.

Surfactant exchange route for composite materials synthesis

We developed a modified polymerization process, in which stacac was a polymerizable monomer that was added to preformed MNPs (Scheme 2).

The MNPs were prepared using literature methods from the $Fe(acac)_3$ precursor.[11] These particles were treated with excess stacac to aid in forming a polymer matrix. The ratio of monomer to nanoparticles was optimized so that a material could be prepared with a dense-packing of nanoparticles. We found that combining 50 mg of MNPs in ethanol with 300 μmol of stacac in a Teflon mold gave a viscous solution that could be polymerized in the presence of AIBN and heat. The product from this reaction was a monolithic material that could adopt the shape of the mold. Using less stacac resulted in a powdery material that was qualitatively similar to pure nanoparticles, whereas using more stacac produced a monolith with a low density of nanoparticles. To demonstrate the ability to form 3-D structures with this material, a toroidal-shaped Teflon mold was used and magnetic toroids were prepared (Fig. S1†).

Characterization of MNP-composite material

The FTIR spectra of the MNP-composite material confirmed that the polymeric nature of the material was originating from stacac. The material had peaks between 1300 and 1800 cm^{-1}, which are similar to the features found for the stacac monomer (Fig. 1). TEM images of the MNP-composite material showed a

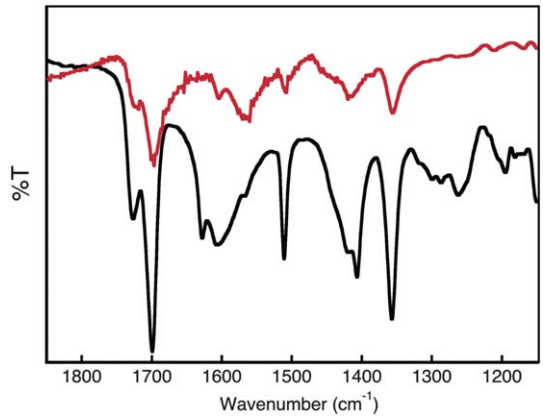

Fig. 1 Infrared spectra of MNP-composite material after polymerization (red), and stacac monomer (black).

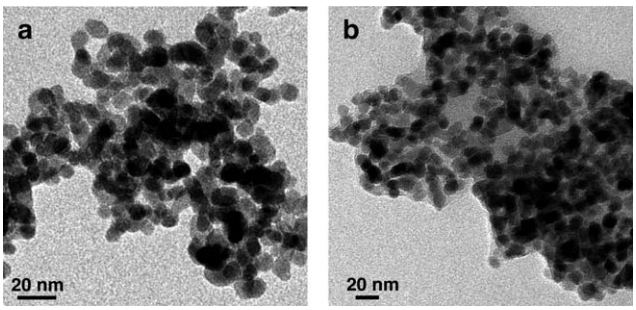

Fig. 2 TEM images of MNPs (a) and MNP-composite material (b).

polymer film surrounding the nanoparticles, but otherwise the shape and size of the nanoparticles were unchanged. A darker gray area in between the particles can be seen, which was not present in the MNPs, suggesting a polymer matrix exists between the particles. The physical properties of the MNP-composite were reliably reproducible, forming 3-dimensional structures resembling the mold used in polymerization. Fig. 2 shows that the TEM images confirm a high density of nanoparticles were present.

X-ray diffraction (XRD) analyses were done to verify that the composite materials still contained crystalline Fe_3O_4. The XRD pattern of pure MNPs (Fig. 3) and the pattern of the MNP-composite have the same peak ratios, and the 2θ values for the major peaks matched those of Fe_3O_4 from the literature.[11–14]

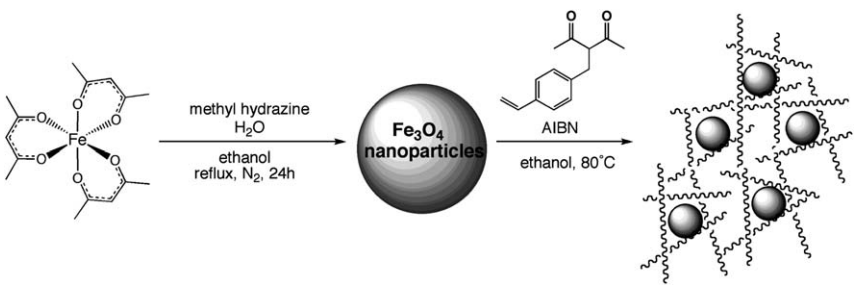

Scheme 2 Preparation of MNP-composite material from $Fe(acac)_3$.

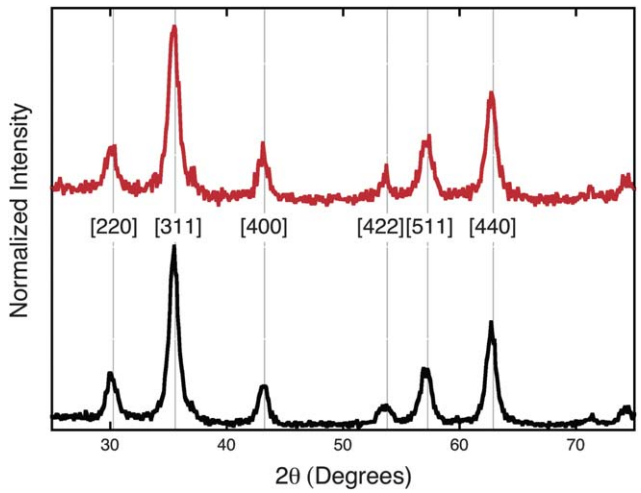

Fig. 3 XRD data of Fe_3O_4 (black) and MNP-composite material (red). Some of the major peaks for bulk Fe_3O_4 are highlighted with grey lines in the figure (PDF#01-087-2334).

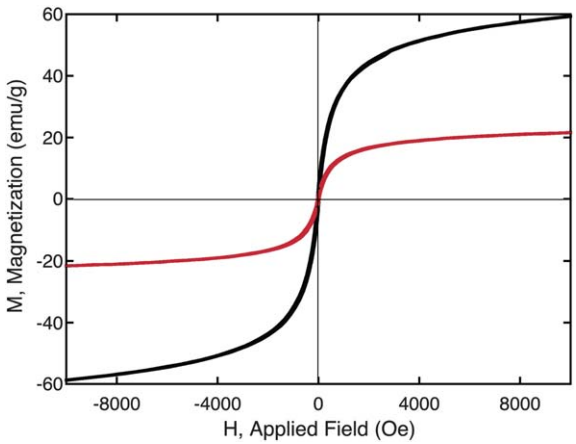

Fig. 4 Magnetization data at 300 K for MNPs (black) and MNP-composite material (red) from −10 000 Oe to 10 000 Oe.

These data provide evidence that the composite materials still contains crystalline Fe_3O_4. The VSM data for the MNP-composite material showed approximately 1/3 the saturation magnetization of the pure MNPs, with $M_{sat} = 22.97$ emu g^{-1}. Some loss of magnetization is expected when introducing a polymer coating, because the polymer does not contribute to the overall magnetization (Fig. 4). This decrease in magnetization is comparable to other magnetic composite materials that have been made with polymers such as polystyrene,[15] polyurethane,[16] chitosan,[17,18] polypyrrole,[19] poly(methylmethacrylate),[8] poly-L-lactide,[20] and organosilanes.[21] In fact, the M_{sat} value calculated for the MNP-composite is larger than many of the composite materials that utilize Fe_3O_4 nanoparticles.[22–25] Additionally, we have examined the susceptibility (χ), which was 3.26 for the MNP-composite material (Table 1).

Preparation and properties of MNPs with Fe(stacac)$_3$

We also examined the use of Fe(stacac)$_3$ as a precursor to prepare MNPs that could be incorporated into composite materials. This iron(III) complex was synthesized in high purity using the procedure outlined in Scheme S1.† MNPs from Fe(stacac)$_3$ was accomplished by treating the complex with methylhydrazine and water in refluxing ethanol. The isolated nanoparticles had comparable properties to those prepared from other iron precursors. MNPs made from Fe(stacac)$_3$ generated a range in particle size of 5.4 ± 0.8 nm as determined by the Scherrer equation,[26] which was corroborated using measurements made from TEM images (Fig. S2†). The MNPs from Fe(stacac)$_3$ had M_{sat} and χ values of 41.2 emu g^{-1} and 1.72, which are consistent with particles having this diameter.

Table 1 Magnetic data from vibrating sample magnetometry (VSM)

	M_{sat}	χ	H_c (Oe)
Nanoparticles			
MNPs from Fe(acac)$_3$	61.8	7.02	27.6
MNPs from Fe(stacac)$_3$	41.2	1.72	27.0
Composite materials			
MNP-composite from reaction mixture aliquot	4.58	0.19	27.3
MNP-composite material	23.0	3.26	28.4
Nanoparticles with different polymers			
MNPs + styrene	63.6	6.55	26.8
MNPs + EGDMA	41.2	3.68	28.3

Although we have demonstrated that Fe(stacac)$_3$ could be used to synthesize MNPs, we found no evidence that the stacac ligand was associated with the particles. Our synthetic procedures always included washing and drying steps, which we found necessary to ensure isolating pure MNPs. However, under these conditions the particles did not appear to contain measurable amounts of stacac. In particular, there were no features associated with stacac in the FTIR spectra of the isolated MNPs (Fig. 5). Moreover, the nanoparticles from this route showed no indication of undergoing polymerization upon the addition of a radical initiator, 2,2′-azobis(2-methylpropionitrile) (AIBN), even at elevated temperatures.

To examine the role of the stacac ligand in formation of the composite materials, we prepared systems using polymerizable monomers that did not contain a metal binding site. Using the same procedure for ligand exchange, the synthesis of composite

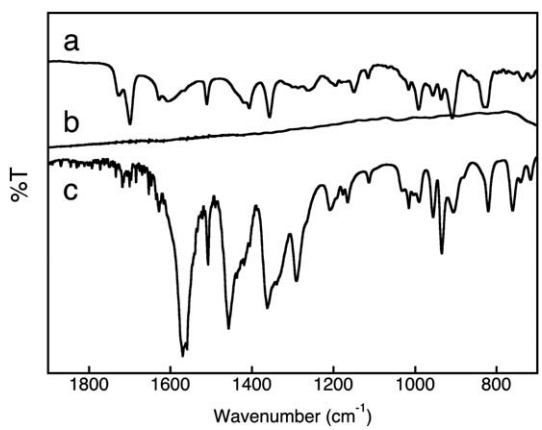

Fig. 5 Infrared spectra of stacac monomer (a), Fe_3O_4 made from Fe(stacac)$_3$ (b), and Fe(stacac)$_3$ (c).

materials was pursued using MNPs and either styrene or ethylene glycol dimethacrylate (EGDMA). The TEM images (Fig. S3†) indicated that these systems were not hybrid materials, but rather mixtures composed of distinct regions of polymer and nanoparticles. For example, when styrene was used as the monomer, a substantially more heterogeneous system was found, in which the nanoparticles were not coated with polymer. The results highlight the need for a metal binding unit on the polymerization monomer to produce composite materials containing densely arranged MNPs. Although the evidence does not suggest that stacac strongly interacts with the MNP surface, stacac with its metal binding site is integral to forming homogeneous materials, in contrast to other functional monomers (*e.g.*, EGDMA) lacking such sites that produced heterogeneous materials. The magnetic properties of these mixtures also have relatively large saturation magnetization and susceptibility values, similar to those observed for pure MNPs. These findings are consistent with essentially nanoparticles with little coating from a polymeric material.

Conclusion

We have described investigations into methods for incorporating MNPs into polymer matrices that utilized stacac, a derivative of the well-known ligand acac. Stacac contains a bidenate metal binding site and a polymerization styryl group, two features that are necessary for making composite materials. One method that utilized $Fe(stacac)_3$ as a synthon produced nanoparticles, yet we were not able to generate composite materials with these MNPs. However, we found that optimizing a surfactant exchange route afforded desired composite materials with a relatively high density of MNPs embedded within a polymeric host. These findings are supported by TEM images, as well as magnetic measurements that showed relatively high magnetic properties. Materials prepared by this method could also be molded into 3-D shapes, as illustrated for a toroid. The surfactant exchange procedure using stacac thus has potential for preparing materials for various applications because of facile processing coupled with superior physical properties.

Acknowledgements

This work is supported by the National Science Foundation (CHE-1057638, RMC) and the University of California-Irvine (ASB). The authors would like to thank Professor Zachary Fisk of UCI Physics for allowing our usage of the Quantum Design MPMS SQUID-VSM in his laboratory. The authors acknowledge the Laboratory for Electron and X-Ray Instrumentation at UCI for the use of the Philips CM-20 TEM.

References

1 T. D. Dunbar, Application: US 7507618 B2, 3M Innovative Properties Company, USA, 2006, p. 12.
2 B. A. Ridley, B. Nivi and J. M. Jacobson, *Science*, Washington, D. C, 1999, vol. 286, p. 746.
3 B. T. Naughton, P. Majewski and D. R. Clarke, *J. Am. Ceram. Soc.*, 2007, **90**, 3547.
4 P. A. Dresco, V. S. Zaitsev, R. J. Gambino and B. Chu, *Langmuir*, 1999, **15**, 1945.
5 S. Lu, J. Ramos and J. Forcada, *Langmuir*, 2007, **23**, 12893.
6 B. Weidenfeller, M. Hofer and F. Schilling, *Composites, Part A*, 2002, **33**, 1041.
7 B. L. Gray, *ECS Trans.*, 2010, **28**, 535.
8 P. Dallas, V. Georgakilas, D. Niarchos, P. Komninou, T. Kehagias and D. Petridis, *Nanotechnology*, 2006, **17**, 2046.
9 R. G. Charles, *Org. Synth.*, 1959, **39**, 61.
10 L. Deng, P. T. Furuta, S. Garon, J. Li, D. Kavulak, M. E. Thompson and J. M. J. Frechet, *Chem. Mater.*, 2006, **18**, 386.
11 K. Hayashi, W. Sakamoto and T. Yogo, *J. Magn. Magn. Mater.*, 2009, **321**, 450.
12 C. Hui, C. M. Shen, T. Z. Yang, L. H. Bao, J. F. Tian, H. Ding, C. Li and H. J. Gao, *J. Phys. Chem. C*, 2008, **112**, 11336.
13 S. Sun and H. Zeng, *J. Am. Chem. Soc.*, 2002, **124**, 8204.
14 M. Arruebo, R. Fernandez-Pacheco, B. Velasco, C. Marquina, J. Arbiol, S. Irusta, M. R. Ibarra and J. Santamaria, *Adv. Funct. Mater.*, 2007, **17**, 1473.
15 L. Jiang, W. Sun and J. Kim, *Mater. Chem. Phys.*, 2007, **101**, 291.
16 M. Ashjari, A. R. Mahdavian, N. Ebrahimi and Y. Mosleh, *J. Inorg. Organomet. Polym. Mater.*, 2010, **20**, 213.
17 B. Feng, R. Y. Hong, Y. J. Wu, G. H. Liu, L. H. Zhong, Y. Zheng, J. M. Ding and D. G. Wei, *J. Alloys Compd.*, 2009, **473**, 356.
18 B. Li, D. Jia, Y. Zhou, Q. Hu and W. Cai, *J. Magn. Magn. Mater.*, 2006, **306**, 223.
19 A. Dey, A. De and S. K. De, *J. Phys.: Condens. Matter*, 2005, **17**, 5895.
20 S. T. Tan, J. H. Wendorff, C. Pietzonka, Z. H. Jia and G. Q. Wang, *ChemPhysChem*, 2005, **6**, 1461.
21 K. R. Reddy, K.-P. Lee, A. I. Gopalan and H.-D. Kang, *React. Funct. Polym.*, 2007, **67**, 943.
22 M. Furlan, B. Brand and M. Lattuada, *Soft Matter*, 2010, **6**, 5636.
23 R. Turcu, A. Nan, I. Craciunescu, O. Pana, C. Leostean and S. Macavei, *J. Phys.: Conf. Ser.*, 2009, **182**, 012081.
24 C. Yang, Y. Guan, J. Xing and H. Liu, *Langmuir*, 2008, **24**, 9006.
25 C. H. Yang, J. J. Du, Q. Peng, R. R. Qiao, W. Chen, C. Xu, Z. G. Shuai and M. Y. Gao, *J. Phys. Chem. B*, 2009, **113**, 5052.
26 B. D. Cullity and S. R. Stock, *Elements of X-Ray Diffraction*, Prentice Hall, Inc., Upper Saddle River, NJ, 3rd edn, 2001.

